Savannah River National Laboratory®

A U.S. DEPARTMENT OF ENERGY NATIONAL LAB • SAVANNAH RIVER SITE • AIKEN, SC • USA

Considerations for Defining G-Values for Aluminum-Clad Spent Nuclear Fuel

Anna L. d'Entremont

September 30, 2024

SRNL-STI-2024-00282, Revision 0

srnl.gov

DISCLAIMER

Printed in the United States of America

Prepared for
U.S. Department of Energy

SRNL-STI-2024-00282
Revision 0

Keywords: radiolysis, aluminum (oxy)hydroxides, G-value

Retention: *Varies (Track number is applicable)*

Considerations for Defining G-Values for Aluminum-Clad Spent Nuclear Fuel

Anna L. d'Entremont

September 30, 2024

Savannah River National Laboratory is operated by Battelle Savannah River Alliance for the U.S. Department of Energy under Contract No. 89303321CEM000080.

REVIEWS AND APPROVALS

AUTHORS:

ANNA D'ENTREMONT (Affiliate) Digitally signed by ANNA D'ENTREMONT (Affiliate) Date: 2024.09.25 17:52:56 -04'00'

Anna L. d'Entremont, Materials Science & Disposition Date

TECHNICAL REVIEWERS:

CHARLES CRAWFORD (Affiliate) Digitally signed by CHARLES CRAWFORD (Affiliate) Date: 2024.09.26 07:31:04 -04'00'

Charles L. Crawford, Glass, Cement, & Ceramic Science Date

APPROVAL:

MORGANA WHITESIDE (Affiliate) Digitally signed by MORGANA WHITESIDE (Affiliate) Date: 2024.09.26 08:00:09 -04'00'

Morgana T. Whiteside, Materials Science & Disposition /Manager Date

JOSEPH MANNA (Affiliate) Digitally signed by JOSEPH MANNA (Affiliate) Date: 2024.09.26 08:26:06 -04'00'

Joseph Manna, Materials Technology & Energy Sciences/Division Director Date

PREFACE

Sealed-canister dry storage of aluminum-clad spent nuclear fuel (ASNF) generated by research reactors is an alternative to current storage and disposition pathways as directed by the U.S. Department of Energy. The major challenge faced for this storage approach is radiolytic H_2 generation, including from the aluminum (oxy)hydroxide layers on the surface of ASNF. Experimental and modeling activities have been carried out to characterize the radiolytic yield as part of a DOE-sponsored research program to develop the technical basis for ASNF dry storage.

The G-value is a commonly way to report results of radiolysis testing and is defined as the radiolytic yield of a species (e.g. molecular hydrogen) per unit radiation energy deposited into the material system. An independent technical review of the ASNF dry storage technical basis performed by Pacific Northwest National Laboratory raised questions about differences in G-value definitions used for experiments on ASNF surrogates consisting of aluminum samples with adherent (oxy)hydroxides compared to G-values reported in prior literature and how the magnitudes compared between different studies.

Material systems resembling ASNF pose complications for measuring/defining G-values to predict the evolution of H_2 in a sealed canister, including i) accounting for radiolytic yields potentially arising from multiple sources, i.e., residual free (vapor), physisorbed, and chemisorbed/chemically bound waters; ii) deciding what portions of the multi-material system to include in the absorbed energy (radiation dose) calculation, considering possible energy exchange between materials as well as measurement limitations, and iii) capturing variations in G-value associated with non-linear yield vs. dose curves and/or dependence on the cover gas.

This report summarizes previous literature information on radiolytic H_2 generation and associated G-values from mixed-material systems (generally oxides in contact with water or organic compounds) and from (oxy)hydroxides/hydrates to compare with the definitions and values for ASNF surrogate samples containing adherent aluminum (oxy)hydroxides.

EXECUTIVE SUMMARY

Radiolytic generation of species such as H_2 is frequently characterized by a "G-value" defined as the amount of a species produced or consumed by radiolysis normalized by the amount of absorbed radiation energy; some of the radiolysis data from research on aluminum-clad spent nuclear fuel (ASNF) dry storage was reported in this format. This report compiles literature information on radiolysis testing and G-values for mixed-material systems (generally oxides with water or organic compounds) or (oxy)hydroxides/hydrates as well as for samples designed to resemble ASNF in order to compare and evaluate factors affecting G-value definitions and testing for these systems.

Despite the seemingly straightforward definition, calculation of G-values for a sample containing more than one material requires a decision of what absorbed energy to use in the calculation, particularly for samples with components that do not undergo radiolysis but may transfer a portion of their absorbed energy to another material and alter its radiolysis behavior. The experimental systems being tested for ASNF dry storage research have some key differences from prior literature that impact how the G-values may be defined due to both practical limitations and theoretical considerations. This report discusses various approaches to G-value definitions used in previous literature, how the radiolytic yields have been defined/reported in the testing of ASNF surrogate samples, reasons for and implications of differences between these definitions, and comparisons between the literature G-values and those in the ASNF research in order to add clarity to the reporting of radiolysis data.

Commonly used approaches for mixed-material systems including one component that breaks down under irradiation and another that does not but may transfer energy (e.g., adsorbed water or organic compounds on oxides) include 1) defining the G-value based on energy deposition in the entire sample and 2) defining the G-value based only on energy deposited directly in the component breaking down under radiolysis. These approaches are prone to over- or underestimating, respectively, the amount of energy actually contributing to the radiolytic yield. G-values based on only a portion of the sample are also sensitive to the quantification of the different components, which can be challenging to measure accurately, particularly for small masses of adsorbed species. Materials such as (oxy)hydroxides and hydrates can both undergo radiolysis to generate H_2 themselves as well as host adsorbed water (physisorbed water), and many cannot survive the high-temperature bake-out processes frequently used to facilitate accurate quantification of the adsorbed species. Both of these characteristics add complications for the calculation of G-values based on only the species undergoing radiolysis.

Some material systems also display non-constant G-values as a function of dose (i.e., non-linear yield vs. dose curves), further complicating the definition and usage of the G-value, since additional absorbed dose may not produce the same radiolytic yield predicted by the cumulative G-value.

As a result, G-values appear to have the most value for application to single components with linear yield vs. dose curves. However, no obvious, straightforward replacement metric exists for more complex systems. It is helpful for experimental studies to include unnormalized radiolytic yields and details of the sample composition/preparation in their reporting in order to enable alternative processing of the data for comparison to other studies or incorporation in models.

G-value magnitudes for ASNF surrogate samples were compared to data from previous literature for mixtures of Al_2O_3 powder with water and for aluminum (oxy)hydroxides in powder form. Some of the literature G-values were converted into different G-value definitions to facilitate more direct comparison. G-values from the ASNF surrogate coupons with adherent bayerite ($Al(OH)_3$) films, normalized by energy deposition in the (oxy)hydroxide film ($G(H_2)_{oxide}$), were up to ~20x larger than G-values for Al_2O_3 powder with adsorbed water calculated based on the total energy deposition in the entire mixture ($G(H_2)_{mix}$) but smaller than G-values based on energy deposition in just the water ($G(H_2)_{H2O}$) for the same Al_2O_3/water

sample. The ASNF surrogates' $G(H_2)_{oxide}$ values were similarly larger than $G(H_2)_{oxide}$ values obtained for boehmite powder under dry or humid argon (based on the mass of the (oxy)hydroxide). Given the differences in the oxide materials (Al_2O_3 vs. AlOOH vs. $Al(OH)_3$) and sample morphology (powders vs. adherent film on metal) and that the $Al(OH)_3$ can also contribute to the radiolytic H_2 yield, the rough magnitudes of these G-values seem to be reasonably consistent.

TABLE OF CONTENTS

LIST OF TABLES

LIST OF FIGURES

LIST OF ABBREVIATIONS

ASNF	Aluminum-clad spent nuclear fuel
DOE	U.S. Department of Energy
DSC	DOE Standard Canister
G(X)	"G-value" (yield per unit absorbed radiation energy) of species X
$G(X)_{mix}$	G(X) from a mixture of materials (e.g., oxide and water) based on energy deposition in the total mixture
$G(X)_{oxide}$	G(X) of a sample containing oxide/(oxy)hydroxide based on energy deposition in the oxide/(oxy)hydroxide only
$G(X)_{H2O}$	G(X) of a sample based on energy deposition in the water only (usually liquid or physisorbed)
$G(X)_{sample}$	G(X) from a solid sample (e.g., a metal coupon with any adherent oxides and adsorbed species) based on energy deposition in the entire sample
$G(X)_{Y}$	G(X) from multi-material system based on energy deposition in species Y only
INL	Idaho National Laboratory
RH	Relative humidity
SEM	Scanning electron microscopy
SNF	Spent nuclear fuel
SRNL	Savannah River National Laboratory
USHPRR	U.S. High Performance Research Reactors

1.0 Introduction

The U.S. Department of Energy (DOE) currently manages a large inventory of aluminum-clad spent nuclear fuel (ASNF) from U.S. High Performance Research Reactors (USHPRR) and some fuel from foreign research reactors in interim storage pending ultimate disposition, with more being generated by currently operating research reactors. The current disposition path for DOE-owned ASNF is chemical dissolution and processing into a vitrified waste form in canisters destined for repository disposal; however, only one processing facility (H-canyon) exists in the USA, and it is currently scheduled for shutdown in 2033 [1], so an alternative disposition strategy is needed for future ASNF that will continue to be generated from the USHPRR.

Dry storage in sealed canisters is an established long-term storage approach for commercial (Zr-clad) spent nuclear fuel (SNF) and is a potential alternative pathway for interim storage and/or disposition of ASNF. Interim storage pending disposition in an SNF repository must be suitable for an extended storage duration (>50 years) since no repository currently exists. DOE has developed designs for a set of DOE Standard Canisters (DSCs) to provide sealed, road-ready dry storage suitable for interim storage, transportation, and potentially disposition of a variety of fuel types in a future repository. Extensive experiments and modeling activities have been carried out by researchers at the Idaho National Laboratory (INL) and Savannah River National Laboratory (SRNL) as part of a DOE-sponsored research program to develop the technical basis for ASNF dry storage, with results to date indicating this storage approach should be safe and viable following suitable drying processes [2].

One of the key challenges identified for sealed dry storage of ASNF is the existence of aluminum (oxy)hydroxide films on the cladding surface formed by corrosion during the fuel's service history, which cannot be readily removed during canister drying due to the elevated temperatures required for thermal dehydration. These (oxy)hydroxides contain significant amounts of chemically bound water, which can potentially break down under irradiation to release H_2 gas during dry storage. Radiolytic generation of species such as H_2 is frequently characterized by a "G-value" reflecting the amount of the radiolysis product generated per unit absorbed radiation dose. An independent technical review of Ref. [2] performed by Pacific Northwest National Laboratory raised questions about the definitions used for radiolysis experiments on aluminum with adherent (oxy)hydroxides compared to G-values reported in prior literature.

The experimental systems being tested to determine ASNF radiolytic yields have some differences from prior literature cited by reviewers which impact how the G-values may be calculated. This report discusses G-value definitions as used in previous literature, how the radiolytic yields have been defined/reported in the testing of ASNF surrogate samples, the reasons for and implications of differences between these definitions, and comparisons between the literature G-values and those in the ASNF research in order to add clarity to the reporting of radiolysis data.

2.0 ASNF dry storage background

2.1 Aluminum oxides and (oxy)hydroxides on ASNF

The aluminum-alloy cladding on ASNF is exposed to liquid water in the reactor and in subsequent wet storage (and, for some types of ASNF, in pre-irradiation "prefilming" procedures), resulting in the formation of adherent oxide/(oxy)hydroxide films on the outer surface of the cladding. Corrosion products relevant to ASNF cladding include alumina (Al_2O_3), the aluminum oxyhydroxide boehmite (AlOOH or $Al_2O_3 \cdot H_2O$), and the aluminum trihydroxide polymorphs bayerite and gibbsite ($Al(OH)_3$ or $Al_2O_3 \cdot 3H_2O$), sometimes in multi-layered and/or mixed oxide films. Other polymorphs of both $Al(OH)_3$ and AlOOH exist but are not commonly reported in studies of aluminum metal corrosion.

Alumina makes up the thin passivation film that forms almost instantaneously on aluminum metal exposed to oxygen, while the (oxy)hydroxides form under exposure to water, either directly from the reaction of water with aluminum metal (releasing H_2) or of water with an existing oxide [3]. The amount and composition of (oxy)hydroxides on the surface of ASNF depend on its history. Laboratory studies of aqueous corrosion of aluminum indicate that the process is complex and depends on multiple variables including temperature/heat flux, pH, coolant flow characteristics, irradiation, and the oxide(s) already on the surface [4], many of which can vary not only from reactor to reactor, but also spatially and temporally over a single fuel assembly. A previous report [4] provides more detail on some of the variables impacting the (oxy)hydroxide formation and summarizing the oxide thicknesses and types reported in post-irradiation examinations of various types of ASNF. Service-formed oxides varied widely in thickness, with reported isolated/local measurements from <1 μm to as high as 80 μm, and showed significant spatial variation over a single element, generally peaking near the middle of the fuel plates with lower thicknesses closer to the edges [4]. Calculated average oxide thicknesses ranged from 12 to 25 μm for the relatively few data sets reporting systematic oxide thickness measurements from different locations on the same plate [4]. The (oxy)hydroxide film morphology includes small-scale structures, resulting in a larger microscopic surface area than the nominal surface area of the cladding or sample.

2.2 Water sources in a dry storage canister

Water in a dry storage canister can exist in the form of free water (liquid or vapor), physisorbed water adsorbed to various surfaces, or chemisorbed/chemically bound water (e.g., incorporated into aluminum (oxy)hydroxides). Prior to storage, loaded SNF canisters are subjected to a drying process, and sealed canisters are backfilled with helium for chemical inertness and effective heat transfer. The removal of water from the canister prior to storage lessens the amount of hydrogen that could be released by radiolysis. Industrial drying processes such as vacuum drying and forced-gas dehydration aim to remove liquid water and reduce water vapor to below a defined threshold (typically 3 Torr (0.4 kPa) partial pressure) [5].

Depending on the temperatures reached during drying processes, some or all of the aluminum trihydroxides ($Al(OH)_3$, bayerite and gibbsite) could be thermally dehydrated, resulting in removal of some of the chemisorbed water [6, 7]. For bayerite, the threshold to trigger this thermal decomposition appears to be 220°C [6, 7]. Boehmite (AlOOH) is not expected to be removed during canister drying due to its higher thermal decomposition temperature. Therefore, a stored canister is expected to contain (oxy)hydroxides: boehmite (service-formed or as a dehydration product of $Al(OH)_3$), aluminum trihydroxides, or a combination thereof, depending on the initial oxide form and the drying conditions.

Radiolytic yields after various drying procedures provide some circumstantial evidence that significant physisorbed water can survive unheated vacuum drying, while elevated temperatures (e.g., 150°C) help to remove it [6]. The amount of physisorbed water likely to remain in the canister is not well established.

3.0 G-value definitions

3.1 Radiolysis and G-values

Ionizing radiation interacts with matter to produce ions and excited molecules, which further react with their surroundings to generate a variety of products, including free radicals and molecular species [8]. This radiation-chemical change is termed radiolysis [8]. This process can be driven by alpha, beta, or gamma radiation, and all produce generally the same ionic and excited states and resulting chemical products but in different proportions due to the differences in their interactions with the absorbing material [8].

In radiation chemistry, the “G-value” is a measure of the radiolytic yield of a substance normalized by the radiation energy absorbed [8]. Historically, it was defined as the number of molecules of the species produced or consumed per 100 eV of absorbed radiation energy; under the SI unit system, it is defined as

moles of the species produced or consumed per joule of absorbed radiation energy, generally expressed in μmol/J (1 molecule/100 eV = 0.1036 μmol/J) [8].

Calculation of the G-value requires quantification of the amount of radiation energy deposited in the material of interest. Absorbed dose quantifies the amount of radiation energy absorbed per unit mass in an irradiated material (SI units Gy = J/kg), and it depends on both the radiation field and the absorbing material [8]. The absorbed dose multiplied by the mass of material provides the absorbed energy which serves as the denominator for the G-value. Radiation dosimetry is used to measure dose and dose rates absorbed by the dosimeter, and the measured values can then be converted to dose experienced by a given sample in the same radiation field [8]. Fricke dosimetry is a common chemical dosimetry method, which measures the accumulation of radiolytic products in an aqueous solution to provide an average absorbed dose over the volume of the dosimeter solution [8].

For a dosimeter and sample of the same size and irradiated under the same conditions, the relationship between the dose in the dosimeter (D_D) and in the sample (D_M) can be calculated based on the mass energy-absorption coefficients (μ_{en}/ρ) as [8]

$$D_M = D_D \frac{(\mu_{en}/\rho)_M}{(\mu_{en}/\rho)_D}.$$

In the range of photon energy where the interaction with matter is dominated by the Compton process, the ratio (Z/A) of atomic number Z to atomic weight A can be substituted for the mass energy-absorption coefficient, i.e., [8]

$$D_M = D_D \frac{(Z/A)_M}{(Z/A)_D}.$$

Laboratory gamma irradiators commonly use Co-60 as the radiation source; the absorption of Co-60 gamma radiation by aqueous systems is well within the Compton region [8], and the same is true for light metals and oxides thereof, including aluminum.

During irradiation of a mixture of different materials, the fraction of the total absorbed energy deposited in each component of the mixture is proportional to its mass fraction and to the "mean mass collision stopping power of the component for the primary and secondary ionizing particles of various energies present in the medium" [8]. The latter quantity is not readily determined, so various approximations have been used, most commonly assuming the components' mass stopping powers are proportional to their Z/A ratios [8]. This assumption results in the following equation for the dose in a component i, where m_i and m_{mix} are the masses of component i and the total mixture, respectively [8]:

$$\frac{D_i}{D_{mix}} = \frac{m_i}{m_{mix}} \frac{(Z/A)_i}{(Z/A)_{mix}}.$$

G-values can be sensitive to experimental conditions, e.g., Petrik et al. [9] noted that the G-value for production of H_2, $G(H_2)$, depends on both primary and secondary processes in radiolysis that can produce or decompose H_2 molecules, which are dependent on the conditions. Their control experiments irradiating water vapor or liquid/vapor mixtures to 0.1–1.5 MGy found that $G(H_2)$ "ranged from 0.1 to 3 $(100\ eV)^{-1}$, depending on the water amount, dose, ampule condition, and other experimental parameters."

3.2 G-value definitions in literature studies of multi-material samples

Since G-values are normalized by absorbed radiation energy, a sample containing multiple materials can complicate the decision of what absorbed energy value to use. This is relevant to a variety of studies that

have shown that species undergoing radiolysis while adsorbed onto or in contact with a material such as an oxide may display significantly different radiolytic yields than when irradiated alone. This phenomenon is frequently attributed to energy transfer between the phases, i.e., energy absorbed in the solid being transferred to the adsorbate is expected to increase radiolytic yield, while energy absorbed in the adsorbate being transferred to the solid is expected to inhibit it.

3.2.1 G-values based on total sample

Early studies by Allen and colleagues [10, 11, 12] of the impact of solid surfaces on radiolysis of adsorbed organic compounds calculated G-values based on the radiation energy deposited in the total sample, i.e., the adsorbed species plus the solid adsorbent powder. This report will denote G-values defined based on energy deposited in the total mixture/sample with the subscripts "mix" or "sample," e.g., $G(H_2)_{mix}$. When data was plotted as a function of the amount of the organic compound in the sample, they also plotted a "liquid line," i.e., a straight line corresponding to the theoretical yield calculated from the energy deposition in just the organic compound and its bulk liquid G-value; comparison to this line facilitated assessment of whether the solid enhanced, inhibited, or had minimal effect on the radiolytic yield [10, 11, 12]. These studies included high-temperature pretreatments of the solid adsorbents to drive off adsorbed species such as water, followed by controlled exposure of the organic compounds.

When the G-values based on total sample absorption [10, 11] or the yield in μmol per unit solid surface area or mass [12] were plotted as a function of the amount of organic compound, most samples showed increasing G-value or yield per unit solid mass/area with increasing fraction of adsorbate at the low end of the adsorbate loading. Some samples showed monotonically increasing G-value/yield over the entire range of adsorbate loadings plotted, while others displayed maxima with subsequent decreases or plateaus [10, 11, 12].

Ref. [12] showed that the G-values for adsorbed azoethane were not necessarily constant for a given system, but instead decreased with increasing total dose. They tentatively attributed this decrease to inhibition of energy transfer by accumulating radiation defects in the solid, supported by, e.g., the observation that irradiating the solid prior to introducing the adsorbate produced a similar lowered G-value, although they noted that some of the observations remain unexplained [12]. They also noted that the fraction of the adsorbed azoethane decomposed was <1% for most experiments [12], suggesting that the decrease did not reflect depletion of the adsorbate.

Other researchers have also used this G-value definition. Hentz [13] reported G_{mix}-values for isopropylbenzene on silica-alumina, including both irradiation of silica-alumina with adsorbed isopropylbenzene and breakdown of isopropylbenzene on previously irradiated silica-alumina. When plotted as a function of dose, the yields (in molecules per gram of solid) did not increase linearly over the range of dose and instead leveled off or displayed more complex changes in slope, indicating the corresponding G_{mix}-values would not be constant with increasing dose. (In this case the percentage of adsorbate decomposed was estimated to reach up to ~70% [13].) LaVerne's [14] study of radiolysis of water on UO_2 reported their yields as both $G(H_2)_{mix}$ (denoted as "Total $G(H_2)$" and as G-values based on energy deposited in just the water.

3.2.2 G-values based on the (single) species undergoing radiolysis

Another approach found in the literature is defining G-values based on only the energy directly deposited into the species that breaks down under radiation, e.g., water or an organic compound, and excluding the energy originally deposited into other species in the irradiated system, e.g., oxide particles. Under this approach, a direct comparison of the G-value to that of the bulk substance provides a straightforward indication of whether there is significant net energy transfer between the materials based on whether it is higher, lower, or roughly equal to the bulk G-value. However, in a system with net energy transfer, it either over- or underestimates the actual amount of energy input that contributes to the radiolysis by ignoring the

transferred energy. This report will denote such G-values by a subscript denoting the species included in the energy calculation, e.g., $G(H_2)_{H2O}$ for yield of H_2 based on the energy deposited in the water only.

G-values defined based on energy in water only have been used as the primary G-value definition in multiple studies of water radiolysis by LaVerne and colleagues, e.g., [15, 16, 17, 18], as well as by other research groups, e.g., Petrik et al. [9]. Ref. [17] stated that only energy deposited in the water was included "since that is where the H_2 originates." Ref. [14] reported $G(H_2)_{H2O}$ in addition to $G(H_2)_{mix}$ data. Reiff and LaVerne [17, 18] applied this approach to both adsorbed water on oxide powders (copper oxides [17] and Al_2O_3 [18]) and also for water/oxide slurries up to 90wt% water.

Reiff and LaVerne's [18] reported G-values as a function of water mass fraction for water/Al_2O_3 slurries with 5–90wt% water showed that $G(H_2)_{H2O}$ peaked near the lowest water fractions tested (~1.3 molecules/100 eV at 5%–10%) and then decreased with increasing water percentage, with the reported bulk water $G(H_2)$ being the lowest. (The bulk water value seems to be a literature value, since no 100% water experiment was described.) The reported $G(H_2)_{H2O}$ for adsorbed water amounting to 0.1wt% of the sample was 80±20 molecules/100 eV, much higher than any of the slurry values. Tests of water on CeO_2, ZrO_2, and UO_2 [15, 14] showed similar dramatic increases in $G(H_2)_{H2O}$ as the adsorbed water content decreased towards zero.

This is very different behavior than was shown for G_{mix}-values in [10, 11, 12], which generally decreased as the fraction of species undergoing radiolysis approached zero (i.e., the sample mass is dominated by the "inert" component). The difference between the two G-value definitions tends to drive this apparent behavior difference even if the underlying data is the same. Refs. [15, 14] demonstrate this by plotting both $G(H_2)_{H2O}$ and $G(H_2)_{mix}$, showing that $G(H_2)_{mix}$ increased with increasing water loading. If energy transferred from the solid to the adsorbed species drives radiolysis, then as the amount of adsorbed species approaches zero, $G_{adsorbed}$ will become very large since most of the energy driving the radiolysis is not deposited directly in the adsorbed layer, while G_{mix} will become small since there is very little material to break down but a relatively large "inert" volume to absorb energy.

3.2.2.1 Adsorbed water quantification

G-values calculated based on energy deposition in just the species undergoing radiolysis are sensitive to the quantification of that species. Radiolysis studies of adsorbed species (even many that use the total mass for G-values) often include a high-temperature pretreatment of the solid to eliminate existing adsorbed species (including contaminants, e.g., adsorbed water in a study of another compound) prior to a controlled exposure to the species of interest [9, 10, 11, 12, 14, 18]. Elimination of pre-adsorbed species facilitates measurement of weight changes during adsorption as a way to quantify of the adsorbed species [14, 18], and the solid adsorbents are generally in the form of powders with large specific surface area, making the sample mass changes associated with monolayers of adsorbate more readily detectable. Some studies also included characterization of the adsorption layers on samples of the same powder and same preparation used for the irradiated samples by methods such as temperature programmed desorption or diffuse reflectance infrared Fourier transform spectroscopy at different temperatures [18].

Previous studies have noted challenges in accurately quantifying the adsorbed layer and have fallen back on the $G(H_2)_{mix}$ definition as a more robust measurement. Refs. [14, 17] noted high uncertainties (20-30%) in some of their reported water loadings due to the small masses of water relative to the oxide making them difficult to measure accurately (e.g., ~2 g samples with water content estimated to be <0.1wt% [14]); as a result, they reported yields in $G(H_2)_{mix}$ as well as $G(H_2)_{H2O}$.

Ref. [14] used a 48-h, 500°C bakeout to eliminate water and contaminants for CeO_2 and ZrO_2 samples due to their stability at high temperatures but limited the bakeout temperature to 100°C for UO_2 samples to avoid oxidation to U_3O_8. They acknowledged that some adsorbed water likely survived the 100°C treatment,

which would result in underestimation of the water loading and consequently overestimation of $G(H_2)_{H2O}$ [14]. In fact, even after 500°C, 48-h drying of ZrO_2, they still measured non-zero radiolytic yield, with a $G(H_2)_{mix}$ only slightly below that for samples prepared at low humidities; this was attributed to some strongly-bound water surviving the bakeout process and being responsible for a large fraction of the radiolytic yield on ZrO_2 [14]. A longer bakeout for ZrO_2 (72 h at 500°C) and less severe bakeouts for CeO_2 (only 24 h at 500°C) did eliminate the observable H_2 yields, suggesting successful removal of adsorbed water [14].

3.2.3 Radiolytic yields of (oxy)hydroxides and hydrates

Unlike the oxides in the studies in Sect. 3.2.1 and 3.2.2, which contain no hydrogen and could only influence the radiolysis of other materials, (oxy)hydroxides and hydrates can themselves produce radiolytic H_2.

LaVerne and Tandon [19] studied radiolytic yields from several hydrates and hydroxides in powder form: $CaCl_2 \cdot 2H_2O$, $CaCl_2 \cdot 6H_2O$, $Ca(OH)_2$, $MgCl_2 \cdot 2H_2O$, $MgCl_2 \cdot 6H_2O$, and $Mg(OH)_2$. Ref. [19] states that radiation chemical yields/G-values "are traditionally given in units of molecules of product per 100 eV of total energy deposited in the medium" and appears to treat all of these compounds as single components, i.e., the mass of waters of hydration or chemically bound water is not assessed separately as adsorbed water was in studies of oxides and water, e.g., [15, 14, 16, 17, 18]. To remove adsorbed water, the hydroxides were baked out at 100°C for 24 h, while the hydrates were dried at room temperature under vacuum or in a drybox with a desiccant, because drying at 100°C "often resulted in the loss of waters of hydration" [19]. Therefore, the G-values in this study appear to be G-values based on the mass of the hydroxide or hydrate.

Most of the $G(H_2)$ values reported for the solid hydroxides and hydrates under gamma radiation are lower than the 0.45 molecules/100 eV cited for bulk water, ranging from 0.042 molecules/100 eV for $MgCl_2 \cdot 6H_2O$ to 0.20 molecules/(100 eV) for $CaCl_2 \cdot 2H_2O$ and $Ca(OH)_2$ [19]. The exception is $MgCl_2 \cdot 2H_2O$, which had an initial $G(H_2)$ of 0.72 molecules/100 eV, decreasing to 0.51 molecules/100 eV by the end of the irradiation (~28 J deposited energy) [19].

Westbrook et al. [20] measured yields from aluminum (oxy)hydroxide powders (≤100 μm particle size): boehmite (AlOOH) and gibbsite ($Al(OH)_3$). The powders were oven-dried at 60°C for 24 h and then tested under either dry cover gas or cover gas with a specified humidity [20]. (This is a relatively low-temperature and short drying treatment compared to those used in other studies.) Yields were not reported as G-values, but instead are reported or plotted as the volume percentage of H_2 accumulated in the gas space for a specified mass of (oxy)hydroxide powder, cover gas condition, and dose. Based on the fill conditions specified (8.2 mL volume, filled to 1 atm, assuming 25°C as specified for initial testing) and the 2.4-g sample mass, the fitted line for "dry boehmite" (irradiated under dry argon) appears to correspond to a $G(H_2)_{oxide}$ of roughly 0.01 μmol/J (0.1 molecules/100 eV) and the fit for "wet boehmite" (irradiated under 85% RH in argon) to roughly 0.005 μmol/J (0.05 molecules/100 eV); the yield of "dry gibbsite" was too low to quantify from the plot.

3.2.4 Other expressions for radiolytic yield

Some studies reported yields in other forms, either in addition to or instead of G-values.

Petrik et al. [9] reported in-text G-values, but primarily plotted their results as the total yield of H_2 (μmol) for samples of specified size/preparation or in arbitrary units providing a relative comparison of similar samples differing in a specific variable. They also plotted yields per unit mass of oxide (μmol/g) and as a function of the oxide's specific surface area (m^2/g) to determine how the yields scaled with powder geometry, concluding that the yield was directly proportional to the solid's surface area [9]. This is consistent with the interpretation of interfacial energy transfer if the distance of energy migration is smaller than the solid particles so that only a thin region of the solid contributes; Petrik et al. estimated the energy migration distance for the ZrO_2 to be ~5 nm [9].

Similarly, many of the radiolytic yields in Ref. [12] were not plotted in terms of G-values, but instead as μmoles per unit surface area or per unit mass of the solid as a function of the ratio of adsorbant to solid, for the same type of solid and same dose to the sample. (For a constant absorbed dose to the total sample, this data is directly proportional to the G-value.) When plotting yields as a function of dose, Hentz reported them in molecules per gram of solid [13].

Yamamoto et al. [21] reported yields from mixtures of water with small quantities of Al_2O_3 or TiO_2 (>99% H_2O) in the form of relative yields normalized by the yield of either a control measurement for water without oxide or by another base case. This approach facilitates easy assessment of the impact of the variable tested, but the lack of quantitative yield information makes it difficult to compare to other studies. The only quantitative yield reported was an in-text statement that the maximum H_2 yield from a given figure "corresponds to $1.8x10^3$ H_2-molecules an incident primary γ-photon" [21]. Assuming this means the H_2 yield per the average energy input of a Co-60 photon, i.e., 1.25 MeV, this would convert to a yield of ~0.14 molecules/100 eV = 0.015 μmol/J for water with α-Al_2O_3, implying the yield of just water (reported to be ~1/8 of the yield for the Al_2O_3 mixture) was ~0.018 molecules/100 eV = 0.0019 μmol/J.

Follow-up work by the same research group [22] reported yields in μmol H_2 for specified sample quantities and dose, and the absorbed dose was explicitly evaluated based on absorption by the water, because the mass of the oxide particles was far smaller than that of the water (<0.2wt%). Their data suggested that the H_2 yield for water with different-size TiO_2 particles was a function of the total surface area of the oxide in solution with minimal impact of particle size for most of the powders tested (7–30 nm nominal particle size), with the exception being much lower yield from the largest particles (200 nm) [22]. They included a plot comparing yields (in μmol) from a control water sample and mixtures with oxides at 10.5 kGy dose, which indicated $G(H_2)$ values on the order of 0.006 μmol/J (0.06 molecules/100 eV) for 100% water and $G(H_2)_{H2O}$ of ~0.05 μmol/J (0.5 molecules/100 eV) for 0.5 g of 33-nm Al_2O_3 particles in 50 g water.

3.3 ASNF dry storage experiments

Materials in ASNF dry storage research samples include aluminum metal, adherent aluminum (oxy)hydroxide films, adsorbed/physisorbed water, and sometimes water vapor, adding several additional complexities beyond the oxide-water systems discussed previously:

- (Oxy)hydroxides contain hydrogen and can potentially undergo radiolysis themselves to release H_2 in addition to potentially exchanging energy with adsorbed water.
- Aluminum (oxy)hydroxides thermally decompose at elevated temperatures, e.g., at ~220°C for bayerite ($Al(OH)_3$), one of the commonly observed (oxy)hydroxide phases on ASNF. Therefore, samples with aluminum trihydroxides cannot be baked out to very high temperatures to ensure removal of physisorbed water and facilitate measurement of water readsorption without fundamentally altering the sample.
- The surface-area-to-mass ratio of coupons is much smaller than that of fine oxide powders, so for a given water coverage (in monolayers), the mass fraction of water on the sample is much smaller and more difficult to measure.
- Net H_2 yield has been measured from so-called "pristine" coupons that were not deliberately corroded to produce an (oxy)hydroxide film, presumably attributable to physisorbed water.

Previous work towards development of a technical basis for extended ASNF dry storage [2] has used two main approaches for computing $G(H_2)$:

1. *$G(H_2)_{oxide}$ based on energy deposited in the (oxy)hydroxide film.* The mass of the oxide/(oxy)hydroxide can be estimated from the mass gain during corrosion or its average thickness combined with the type of (oxy)hydroxide. This definition directly accounts for one of the primary hydrogen-containing materials in the sample and excludes the energy deposited in the metal substrate (which could potentially exchange energy with the oxide or water). It does not explicitly account for the adsorbed water, but the amount of adsorbed water is expected to be very small compared to the (oxy)hydroxide for most corroded samples. $G(H_2)_{oxide}$ cannot be defined for a sample without a quantifiable amount of oxide.

2. *$G(H_2)_{sample}$ based on the total sample mass (aluminum metal, (oxy)hydroxide, and water).* This is simple to measure and can be used for samples with and without oxide films or adsorbed water, but is expected to include a significant amount of radiation energy that does not participate in the radiolysis process due to the relatively large sample volume, skewing $G(H_2)_{sample}$ towards lower values.

In theory, $G(H_2)_{H2O}$ based on the mass of (physisorbed) water could also be applied to these samples. This would be directly equivalent in definition to $G(H_2)_{H2O}$ in Sect. 3.2.2. However, quantification of the small amounts of adsorbed water for metal coupons with (oxy)hydroxides would be even more difficult than for the oxide samples described previously, and this definition ignores the (oxy)hydroxide itself as a potential source of radiolytic H_2.

Unfortunately, trying to account for all of the contributing energy deposition including energy transfer is complex and likely system-dependent. In a multi-component system of aluminum metal, one or more (oxy)hydroxide types, and water, it is difficult to determine:

- *What fraction of the radiolytic H_2 comes from what source*? Potential H_2 sources that might generate different G-values/yield behavior in the same system include water vapor, boehmite (AlOOH), trihydroxides ($Al(OH)_3$), and physisorbed water adsorbed to various surfaces. Particularly for physisorbed water, it seems likely that the G-values/yield behavior will depend on both the properties of the substrate (e.g., aluminum, alumina, or any of the (oxy)hydroxides) and the coverage/loading of physisorbed water.

- *What portions of the sample contribute to the radiolysis by energy transfer?* Some portions of the sample are most likely too distant from the adsorbed water (and/or (oxy)hydroxide) to contribute to its radiolytic breakdown, and calculating $G(H_2)_{sample}$ using the full mass of the sample therefore lowers the G-value due to the energy deposition in a way that may not transfer to a system with different relative amounts or different geometry of metal, (oxy)hydroxide, and water.

4.0 Discussion

4.1 Comparison of ASNF radiolysis experiments to literature data

Reviewers requested that the $G(H_2)$ values measured for aluminum samples be converted into $G(H_2)_{H2O}$ values to enable direct comparison with the values reported by Reiff and LaVerne [18] for Al_2O_3 and water. However, there are several differences in the material systems that make this specific conversion infeasible.

The first challenge is accurate quantification of the (small) amount of physisorbed water on the surface. This information is not available for the aluminum coupon samples. Reiff and LaVerne [18] were able to measure this because their material system was Al_2O_3 particles that could be baked to high temperatures (500°C) and weighed during readsorption of water. Applying this kind of high-temperature bakeout to samples with aluminum trihydroxides in their surface films would thermally decompose some or all of the $Al(OH)_3$, fundamentally altering the material system being tested. In addition, the Al_2O_3 samples were fine

powder, while the ASNF surrogate samples consist of aluminum metal coupons with or without adherent (oxy)hydroxide films; as a result, these samples have much lower specific surface area to physisorb water, and the mass of physisorbed water would be very small and difficult to measure from changes in the much larger sample mass.

A second challenge is the conceptual question of which materials participate in the radiolysis process itself. Al_2O_3 itself contains no hydrogen and therefore cannot have its own $G(H_2)$; it can only influence the radiolytic breakdown of the water. The aluminum (oxy)hydroxide films do contain hydrogen and are expected to be a participating medium that may undergo radiolytic breakdown with its own contribution to the H_2 yield as well as potentially exchanging energy with the metal and/or physisorbed water.

However, the data given in Ref. [18] can be converted into approximate $G(H_2)_{mix}$ values for their entire Al_2O_3 and water mixture for a closer comparison.

4.1.1 Reiff and LaVerne $G(H_2)_{H2O}$ converted to $G(H_2)_{mix}$ (based on water + Al_2O_3)

Table 4-1 converts the $G(H_2)_{H2O}$ values reported by Reiff and LaVerne [18] and based on the energy deposition in the water only into $G(H_2)_{mix}$ values based on energy deposition in the total slurry of Al_2O_3 plus water. The values reported in the original paper are given in column 2 of Table 4-1; the values for 5%–90% H_2O slurries and for 100% H_2O were digitized from Fig. 3 of Ref. [18], while the value for 0.1% H_2O adsorbed onto the oxide came from the text of Section 3.2 of that paper. (The uncertainties/error bars have not been included here.) Note that the 100% H_2O $G(H_2)$ value appears to be a literature value, since the experimental descriptions do not mention a test with 100% H_2O, only the tests with adsorbed water (~0.1% H_2O) and 5–90% H_2O slurries [18].

For a slurry with mass fraction m_{H2O} of H_2O, the energy E_{Al2O3} deposited in the Al_2O_3 per 100 eV deposited in the H_2O was calculated as

$$E_{Al2O3} = \frac{1 - m_{H2O}}{m_{H2O}} \frac{(Z_{Al2O3}/A_{Al2O3})}{(Z_{H2O}/A_{H2O})} (100\ eV)$$

where Z is the sum of the atomic numbers and A is the sum of the mass numbers of the molecule's atoms, i.e., $Z_{Al2O3}/A_{Al2O3} = [2(13) + 3(8)]/[2(27) + 3(16)] = 0.49$ and $Z_{H2O}/A_{H2O} = [2(1) + 8]/[2(1) + 16] = 0.56$. The converted $G(H_2)_{mix}$ is then calculated as

$$G(H_2)_{mix} = G(H_2)_{H2O} \frac{100\ eV}{100\ eV + E_{Al2O3}}.$$

Table 4-1. Conversion of $G(H_2)_{H2O}$, reported in Reiff and LaVerne [18] and based on energy deposition in the water only, to $G(H_2)_{mix}$ based on energy deposition in the total slurry (Al_2O_3 plus H_2O), in both the original units of molecules/100 eV and in µmol/J.

H_2O mass percentage	Reported $G(H_2)_{H2O}$ (molecules/ 100 eV)	Energy deposited in Al_2O_3 per 100 eV inH_2O (eV)	Total energy in slurry per 100 eV in H_2O (eV)	Converted $G(H_2)_{mix}$ (molecules /100 eV)	$G(H_2)_{H2O}$ (µmol/J)	$G(H_2)_{mix}$ (µmol/J)
0.1%	80	88147.06	88247.06	0.09	8.3	0.009
5%	1.22	1676.47	1776.47	0.07	0.126	0.007
10%	1.28	794.12	894.12	0.14	0.133	0.015
20%	1.02	352.94	452.94	0.23	0.106	0.024
40%	0.89	132.35	232.35	0.38	0.092	0.039
60%	0.81	58.82	158.82	0.51	0.084	0.053
80%	0.78	22.06	122.06	0.64	0.081	0.066
90%	0.8	9.80	109.80	0.73	0.083	0.076
100%*	0.45	0.00	100.00	0.45	0.047	0.047

*100% G-value may be a literature value rather than measured in [18].

The converted values from Table 4-1 are plotted in Figure 4-1. The conversion makes no change in the value for 100% H_2O (0.45 molecules/100 eV), while the values for all other data points decrease, as expected due to accounting for the additional energy deposition in the Al_2O_3. The significant increase in G-value from 100% H_2O to 90% H_2O remains for both definitions of the G-value, but for most of the range of slurry compositions, the converted $G(H_2)_{mix}$ values in Figure 4-1 increase with increasing H_2O fraction (presumably because more of the total energy contributes to water radiolysis by either direct energy deposition or energy transfer rather than remaining solely in the Al_2O_3) rather than decreasing with increasing H_2O fraction as it appears for $G(H_2)_{H2O}$ based on energy deposition in water only.

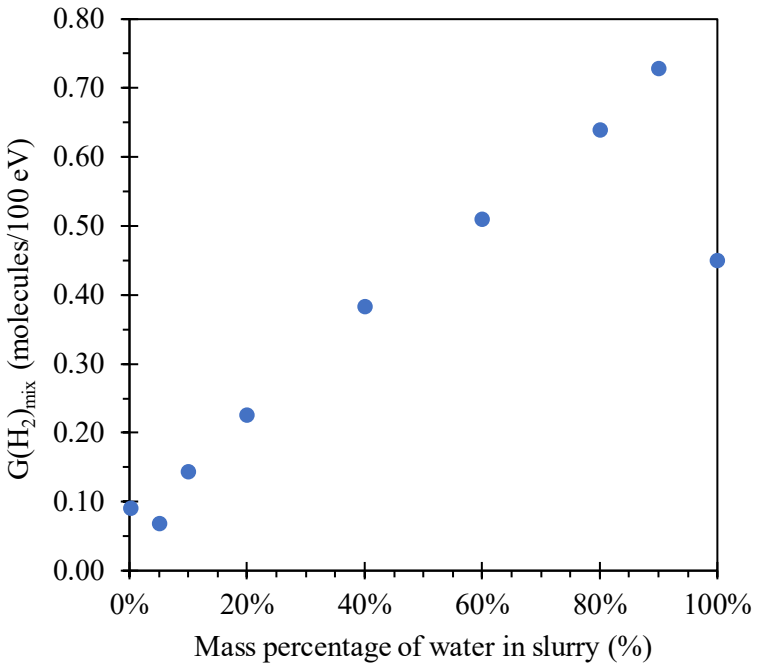

Figure 4-1. G(H_2) converted from [18] to values based on total energy deposition in Al_2O_3 + H_2O slurry, as a function of the mass percentage of H_2O.

Notably, normalizing by the total energy nearly eliminates the massive jump that appeared in the reported $G(H_2)_{H2O}$ at the low-H_2O end of the range as the H_2O fraction decreased from 5% to only 0.1%. When normalized by the total energy, the calculated $G(H_2)_{mix}$ values for adsorbed water (0.1%) and the 5% H_2O slurry are very similar. The jump to the originally reported 80±20 molecules/100 eV (in H_2O) is presumably an artifact of the fact that vastly more energy was available as energy transfer from Al_2O_3 than was deposited directly in the H_2O, and the original $G(H_2)_{H2O}$ calculation had no way to incorporate this energy input.

4.1.2 Radiolysis from corroded aluminum coupons

Parker-Quaife et al. [23] reported H_2 yields from corroded aluminum alloy 1100 (AA1100) coupons under various cover gases (air, Ar, and N_2), each with several relative humidities (approximately 0%, 50%, and 90–100% RH). The coupon dimensions were 2.5 cm × 0.65 cm × 0.15 cm [23], corresponding to 0.66 g at the 2.71 g/cm^3 density of aluminum. Corrosion mass gains ranged from ~3.6–3.9 mg [23], corresponding to an estimated ~5.4–5.9 mg of bayerite[1]. The average thickness of the (oxy)hydroxide films, as estimated from the corrosion mass gain and measured from scanning electron microscopy (SEM) cross-section images, was 5–6 μm, and the (oxy)hydroxide was found to be predominantly bayerite ($Al(OH)_3$) [23]. The samples were gamma-irradiated in glass ampoules to doses ranging from 0.5–1.0 MGy [23].

H_2 yields were reported as quantity of H_2, $G(H_2)_{sample}$, and $G(H_2)_{oxide}$, along with information on the corrosion weight gains, oxide thicknesses, etc. Not enough information is available to quantify the physisorbed water on the samples. The yields reported for ambient-temperature tests under argon are reproduced in Table 4-2. The $G(H_2)_{sample}$ values, which are dominated by energy deposition in the metal coupon due to its large mass compared to the oxide, were very small, i.e. 0.0065 to 0.0108 molecules/100

[1] The corrosion mass gain corresponds to the mass of oxygen and hydrogen added to the sample, so the total mass of bayerite can be calculated based on the molecular weights (MW) as: Estimated bayerite mass = (Corrosion mass gain) $\frac{\text{MW of Al(OH)}_3}{\text{MW of (OH)}_3}$.

eV (0.00067 to 0.00112 μmol/J), while the $G(H_2)_{oxide}$ values were more than two orders of magnitude higher at 1.12 to 1.88 molecules/100 eV (0.116 to 0.195 μmol/J).

Table 4-2. Radiolytic yields reported for aluminum coupons with bayerite films under argon and different humidities [23]. The G-values are reported in two forms: $G(H_2)_{sample}$ based on energy deposited in the entire sample (total mass ~0.66 g) and $G(H_2)_{oxide}$ based on energy deposition in only the (estimated) oxide mass (less than ~6 mg).

Cover gas	relative humidity (%)	absorbed gamma dose (kGy)	H_2 production (μL)	$G(H_2)_{sample}$ (molecule/100 eV)	$G(H_2)_{oxide}$ (molecule/100 eV)
Argon	1	537	7.5 ± 0.2	0.0093 ± 0.0003	1.6355 ± 0.0327
	49	543	8.8 ± 0.6	0.0108 ± 0.0007	1.8831 ± 0.0973
	91	558	8.7 ± 0.8	0.0106 ± 0.0010	1.7539 ± 0.1021
	0	1070	10.2 ± 1.2	0.0065 ± 0.0007	1.1155 ± 0.1519
	49	1081	14.2 ± 1.3	0.0088 ± 0.0008	1.4659 ± 0.1509
	93	1110	14.0 ± 1.5	0.0084 ± 0.0009	1.4219 ± 0.1229

The data in Table 4-2 was obtained for samples with potential physisorbed water and (in some cases) humid cover gas, but no liquid water. Therefore, when comparing to Reiff and LaVerne's data (Table 4-1), the lowest-H_2O data point is the most direct comparison in terms of adsorbed water content (the 0.1wt% H_2O loading was achieved by exposure to 53% RH [18]). Reiff and LaVerne's samples did not include a large mass of metal, so it is not surprising that the coupon $G(H_2)_{sample}$ values are lower than the $G(H_2)_{mix}$ values in Table 4-1. Comparing the G-values based on the oxide, the $G(H_2)_{oxide}$ values for the corroded coupons (Table 4-2) are greater than the $G(H_2)_{mix}$ values for the Al_2O_3 + water mixture, and in particular are much greater (12–21x) the $G(H_2)_{mix}$ for adsorbed water (0.1% H_2O). Given that the (oxy)hydroxide is also a potential source of radiolytic H_2 along with the water (unlike the Al_2O_3), there is also an argument for $G(H_2)_{oxide}$ being equivalent to the $G(H_2)_{H2O}$ values from Table 4-1; here, the corroded-coupon $G(H_2)_{oxide}$ values are comparable to $G(H_2)_{H2O}$ for the low-H_2O slurries, e.g., 5-10%, but well below the reported 80 molecules/100 eV reported for 0.1wt% adsorbed water on Al_2O_3. The $G(H_2)_{oxide}$ values in Table 4-2 are also much larger than the $G(H_2)_{oxide}$ yields estimated from the boehmite powder data in [20] (~0.1 molecules/100 eV = 0.01 μmol/J under dry argon and 0.05 molecules/100 eV = 0.005 μmol/J under 85% RH argon, bracketing the low-water $G(H_2)_{mix}$ from Table 4-1). The higher $G(H_2)_{oxide}$ yields for adherent bayerite films on the aluminum coupons compared to Al_2O_3 or (oxy)hydroxide powders may reflect the contribution of energy transfer from the aluminum metal substrate.

Following the radiolysis testing under air, N_2, and Ar [23], similar testing was performed under helium for both AA1100 and AA6061 alloys [24, 25]. Although the same corrosion conditions were used for both alloys, the resulting corrosion mass gain for AA6061 was found to be ~3.4x that for AA1100 [25]. The reported yields in Refs. [24, 25] were normalized based on the total sample, as either $G(H_2)_{sample}$ values (μmol/J) normalized by energy deposition in the sample or normalized by the sample mass (μmol/kg) as a function of dose. The $G(H_2)_{sample}$ values [24] were based on the slope of a linear fit that was *not* constrained to go through a zero intercept, i.e., it captured the local slope of the yield curve region rather than the total cumulative yield and dose.

The $G(H_2)_{sample}$ values for corroded AA1100 under helium up to ~5 MGy were 1.15×10^{-4} to 4.19×10^{-4} μmol/J (1.11×10^{-3} to 4.04×10^{-3} molecules/100 eV) [24] and found to be comparable to those previously measured for AA1100 under N_2, 1.5×10^{-3} to 4.8×10^{-3} molecules/100 eV (1.6×10^{-4} to 5.0×10^{-4} μmol/J) [23], both measured for 0-100% RH. The $G(H_2)_{sample}$ values for corroded AA6061 under helium (up to ~2 MGy dose) were 2.78×10^{-4} and 2.18×10^{-4} μmol/J for 0% and 50% RH, respectively [24].

Irradiation to higher doses (up to ~35 MGy) with 50% RH [25] demonstrated that the yield of H_2 (µmol/kg) for both the AA1100 and the AA6061 did not increase linearly with increasing dose over the full dose range, indicating non-constant G-values. Per Figure 2 of [25], the initial, low-dose yields appeared linear with similar H_2 generation rate, but at higher doses the slopes decreased, and the AA1100 produced a significantly higher yield than AA6061 by ~30 MGy [25].

Figure 4-2 shows $G(H_2)_{sample}$ and $G(H_2)_{oxide}$ values from relatively large, parallel-plate surrogate assemblies made of AA6061 (total sample mass ~600 g, surface area nearly 3800 cm^2) and corroded in room-temperature water to produce bayerite films of 5-10 µm thick; based on the corrosion mass gains of 4.3-5.3 g, the bayerite masses and average thicknesses were estimated to be 7–8 g and 7–9 µm, respectively) [26, 27]. The samples tested several different drying approaches including air-drying only ("As-Corroded No-Vacuum"), extended (12-h) vacuum ("As-Corroded"), and heated drying for 4 h at two different temperatures (150°C As-Dried and 220°C As-Dried); they were then backfilled with dry helium and gamma-irradiated to >15 MGy inside stainless-steel "mini-canisters" with a sampling line to allow repeated gas sampling for the same sample [26, 27]. Note that the G-values here are calculated based on the *cumulative* yield and dose of the data point relative to the origin.

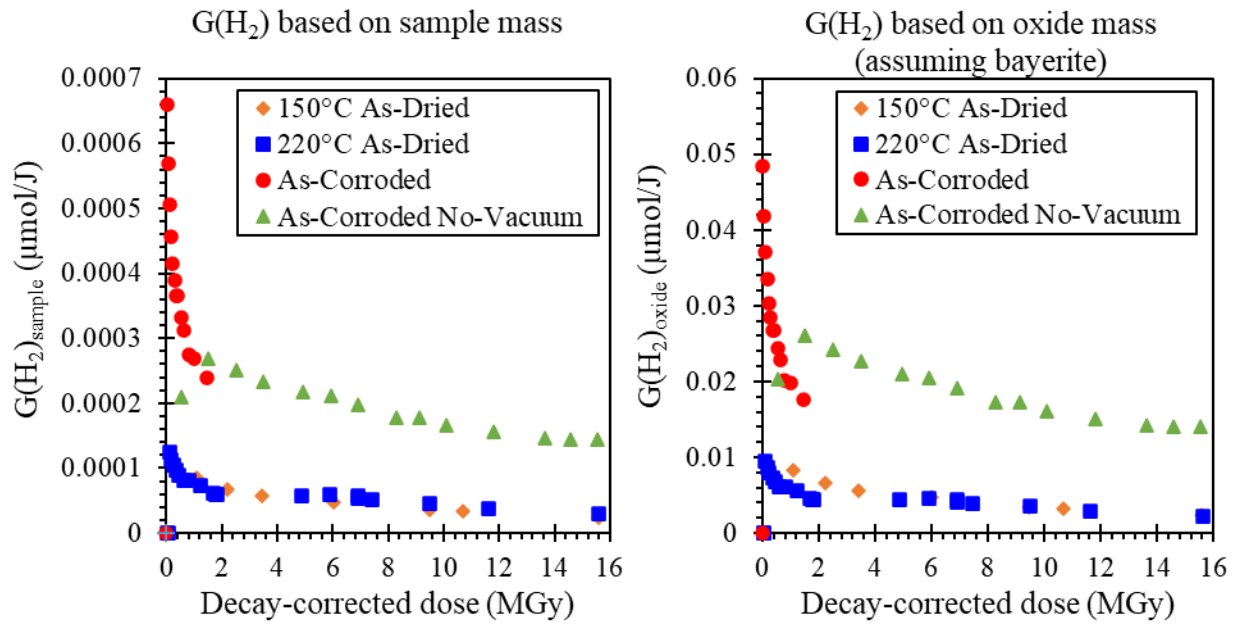

Figure 4-2. G-values from mini-canister radiolysis experiments [26, 27], (left) $G(H_2)_{sample}$ based on the total sample mass and (right) $G(H_2)_{oxide}$ based on the oxide mass (calculated from corrosion mass assuming all bayerite).

The calculated G-values were not constant and peaked in the low-dose <2 MGy range for all four samples; they showed a continuing decrease in G-values at larger doses.

Table 4-3 summarizes ranges of G-values from the mini-canister data and from the ampoule data for corroded aluminum samples. Both the $G(H_2)_{sample}$ and $G(H_2)_{oxide}$ values for the mini-canister tests (under helium) in Figure 4-2 in the low-dose range (<2 MGy) were smaller than the respective $G(H_2)_{sample}$ and $G(H_2)_{oxide}$ values obtained from Ref. [23] under argon up to 1.1 MGy (Table 4-2), but they were of the same order of magnitude. (Note that there were multiple differences between the tests, including coupon alloy, corrosion conditions, cover gas, drying conditions, etc.) The low-dose (<2 MGy) $G(H_2)_{sample}$ values for the mini-canisters ranged from a maximum of 0.00066 µmol/J (for the As-Corroded sample at its lowest dose) down to ~5×10^{-5} µmol/J (As-Dried canisters at ~2 MGy) while $G(H_2)_{sample}$ values from Ref. [23] ranged

from 0.00067 to 0.00112 μmol/J in the ~0.5-1 MGy range, i.e., the highest mini-canister $G(H_2)_{sample}$ was approximately at the lower end of the range for $G(H_2)_{sample}$ in Ref. [23]. Similarly, the low-dose (<2 MGy) $G(H_2)_{oxide}$ values for the mini-canisters ranged from about 0.005 to 0.05 μmol/J, compared to $G(H_2)_{oxide}$ values of 0.116 to 0.195 μmol/J from [23]. The $G(H_2)_{sample}$ values for the mini-canisters at low dose (<2 MGy) were comparable to the ampoule data measured in Ref. [24] for corroded coupons under helium ($\sim 1\times10^{-4}$ to 4×10^{-4} μmol/J).

Table 4-3. Comparison of G-values for tests of aluminum-alloy surrogate samples with adherent (oxy)hydroxides tested in stainless-steel mini-canisters [26, 27] or glass ampoules [23, 24].

Test type	Dose range (MGy)	Alloy	Cover gas	$G(H_2)_{sample}$ (μmol/J)	$G(H_2)_{oxide}$ (μmol/J)
Mini-canisters [26, 27]	< 2	AA6061	He, dry	$\sim 5\times10^{-5}$ to 6.6×10^{-4}	0.005 to 0.05
Ampoule [23]	0.5–1.1	AA1100	Ar, 0-93% RH	6.7×10^{-4} to 1.12×10^{-3}	0.116 to 0.195
Ampoule [24]	<5	AA1100	He, 0-100% RH	1.15×10^{-4} to 4.19×10^{-4}	--
Ampoule [24]	<2	AA6061	He, 0-50% RH	2.18×10^{-4} to 2.78×10^{-4}	--

The mini-canister $G(H_2)_{oxide}$ values are in the same range as the $G(H_2)_{mix}$ from Ref. [18]'s Al_2O_3-water mixtures (Table 4-1). The $G(H_2)_{mix}$ of 0.009 μmol/J for 0.1wt% H_2O adsorbed on Al_2O_3 (Table 4-1) is approximately equal to the initial $G(H_2)_{oxide}$ for the mini-canisters subjected to heated drying (Figure 4-2). The maximum mini-canister $G(H_2)_{oxide}$ of ~0.05 μmol/J was roughly equivalent to $G(H_2)_{mix}$ for Al_2O_3 with 60wt% water and larger than $G(H_2)_{mix}$ for all of the lower-water-content mixtures. The mini-canister $G(H_2)_{oxide}$ values were smaller than the originally reported $G(H_2)_{H2O}$ values from Ref. [18] (except for the 0.45 molecules/100 eV = 0.047 μmol/J value for pure water), and the mini-canister $G(H_2)_{sample}$ values were much smaller, as expected due to the inclusion of all energy deposited in the relatively large aluminum substrate, most of which probably does not participate in the radiolysis.

A review [28] of preliminary radiolysis data from aluminum samples with (oxy)hydroxides, including Ref. [23], attempted to formulate physical explanations for the observed yield behavior, including differences in yield behavior at low dose between Ar and N_2 cover gas (and absence of detectable H_2 generation under air), and the relative H_2 yields from "pristine" coupons with no (oxy)hydroxide film versus coupons with ~5-μm bayerite films. The reviewed data was obtained for three cover gases, Air, N_2, and argon, with relative humidities ranging from nominally zero to ~90%. H_2 generation was not detected for "blank" ampoules containing the cover gas and varying humidity without an aluminum coupon but was detected for ampoules containing unoxidized samples, presumably arising from physisorbed water, as well as for ampoules containing corroded samples.

No detectable H_2 was observed for radiolysis tests under air, but H_2 generation was observed under both N_2 and Ar. The lack of H_2 under air was attributed to free radical scavenging by the O_2 in air (the primary difference between the air and N_2 cover gases) [23]. In the absence of O_2, a cover gas dependence between N_2 and Ar was observed for both oxidized and unoxidized coupons. Yields were smaller under N_2 than under Ar for both sample types and all humidities, and the shape of the yield curve (at least for corroded samples) appeared qualitatively different between N_2 and Ar in the low-dose range: Accounting for the theoretical zero intercept (zero yield at zero dose), the slope of the yield curve appeared to increase with increasing dose under N_2 and decrease under Ar [28]. Despite non-linearity at low doses, yield curves appeared to be linear at higher doses (>500 kGy) with slopes of very similar magnitudes between N_2 and Ar cover gases and between oxidized and unoxidized samples for a given RH (albeit with different non-

zero intercepts for the fits) [28]. In addition, for both sample types/cover gases, the yields for 0-1% RH were lower than those for higher humidities in the same cover gas, while the differences between ~40-50% and 80-90% RH were much smaller [28].

Kesterson et al. [28] postulated that the observed yields (up to ~1 MGy) were dominated by radiolysis of physisorbed water rather than of (oxy)hydroxide, and that the low-dose (<500 kGy) difference in behavior reflected interactions of the radiolytic H_2 with the cover gas, namely radiolytic production of NH_x that effectively suppressed H_2 generation until an equilibrium was established for the chemical reaction. Later experiments [24] showed that yields under helium were lower than under argon and comparable to those under N_2, which was attributed to a different cover gas interaction, i.e., Penning ionization in He promoting decomposition of H_2. Both the lower yields at 0-1% RH and the similarity in slope between the oxidized- and unoxidized-coupon yield curves at >500 kGy doses support the idea that a large fraction of the measured yield originated from physisorbed water [28]. However, the amount of chemically bound water in a ~5-µm (oxy)hydroxide layer far exceeds the amount of physisorbed water expected to be adsorbed on the surface, making it a much larger reservoir for potential radiolytic H_2 release in the long term [28].

The hypothesized yield behavior, illustrated in Figure 4-3, consisted of several regimes: 1) a transient, non-linear regime dependent on interactions with the cover gas, 2) a linear-yield regime (constant generation rate) dominated by yield from physisorbed water until it is depleted, 3) a linear-yield regime with lower generation rate dominated by yield from chemisorbed water (i.e., the water chemically incorporated into the (oxy)hydroxide), and, eventually, 4) a plateau where net H_2 generation ceases due to either full depletion of physisorbed and chemisorbed water or reaching a chemical equilibrium with back reactions [28]. This formulation essentially supposes that the initial transient behavior cannot be captured by a (constant) G-value, and that, at higher doses, two or more generation rates (G-values) are superimposed, i.e., for physisorbed water and for chemisorbed water/(oxy)hydroxide(s), which is expected to result in changes in the effective net G-value for the system as water sources are depleted.

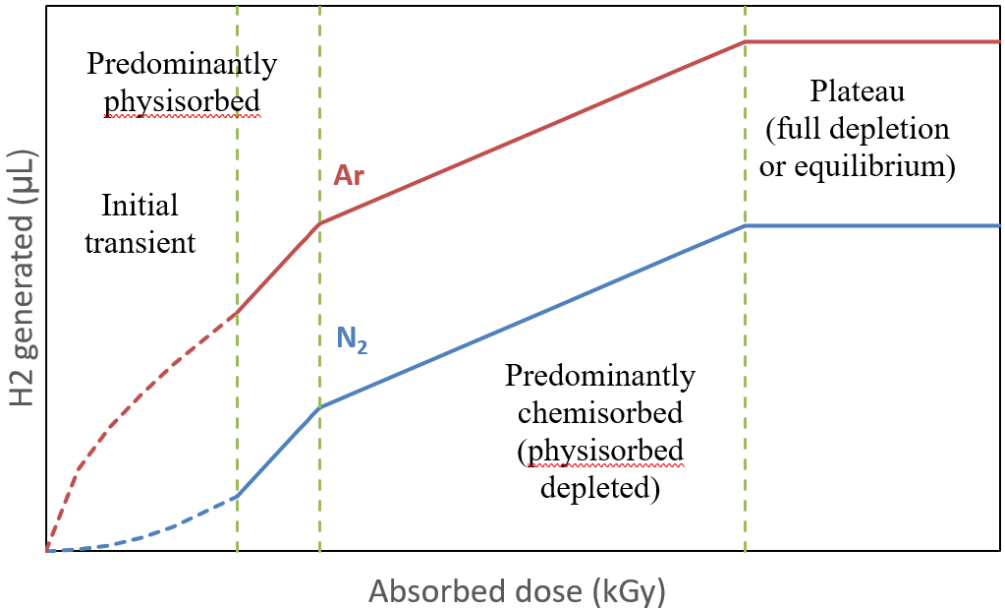

Figure 4-3. Hypothesized yield behavior for H_2 yield from aluminum with (oxy)hydroxides under different cover gases, from [28].

4.2 Generalizability of the G-value

One of the theoretical advantages of a normalized radiolytic yield like a G-value is obtaining a value that can be applied to other systems to predict the radiolytic yield, e.g., predicting radiolytic H_2 from water based on the commonly reported 0.45 molecules/100 eV value. Unfortunately, an experimentally obtained $G(H_2)$ value for a multicomponent system (e.g., oxides and water) with energy transfer cannot necessarily be applied to a system with different proportions of the same materials to predict the correct yield, regardless of whether the $G(H_2)$ is based on energy deposition in the water only or the total sample.

This is readily evident from literature data showing that the G-value varies as a function of the relative amounts of oxide vs. water or other compounds in a sample. Table 4-1 shows that the $G(H_2)$ values measured in [18] were strongly dependent on the composition of the slurry, regardless of whether it is calculated based on energy deposited in the water or in the total slurry, with particularly extreme variation in $G(H_2)_{H2O}$ as the H_2O fraction decreased towards zero. This behavior makes sense, since the $G(H_2)_{H2O}$ values neglect the energy deposited in the Al_2O_3 and transferred to the water, while $G(H_2)_{mix}$ includes energy deposited in the Al_2O_3 that is *not* transferred to the water, and the fraction of transferred versus non-contributing energy will logically vary depending on the relative amounts and likely the geometry of the Al_2O_3 and water. Therefore, using a G-value from a system with different material proportions is likely to under- or overestimate the yield because the fraction of "non-participating" energy deposition changes. Ideally, an accurate and physically relevant $G(H_2)$ value would account for all energy deposition that contributes to the radiolytic H_2 generation without including un-transferred energy, but this would require detailed determination of what parts of the solid can transfer energy to the water and/or (oxy)hydroxide, which currently does not exist.

In addition, existing studies have shown that the G-values for a given system are not necessarily constant as the dose increases. Variation in G-value at different doses adds additional complications to possible G-value definitions. For a constant G-value, the increase in radiolytic yield as a function of dose is linear with its intercept at the origin. G-values calculated based on any two points collected along the linear yield vs. dose curve (or based on a fit of multiple data points) should yield roughly the same value, and such a G-value can be easily used to define a source term/generation rate in a predictive model. However, for a non-linear yield vs. dose curve, the G-value calculated based on the *cumulative* yield and *cumulative* absorbed dose since the beginning of the experiment (i.e., the slope of a line going through the origin and the current data point) will be different than a G-value calculated based on the local slope of the yield curve (i.e., the current generation rate). The local generation rate/relevant source term in a model would correspond more closely to the local slope, and this approach of looking at the local slope of the curve was used, e.g., in Ref. [28] to highlight similarities in longer-term generation rates between different sample conditions when isolated from the initial, short-term differences in behavior.

Given the variability of $G(H_2)$-values depending on experimental conditions [9], recent ASNF radiolysis experiments at SRNL have aimed to use experimental conditions that provide a "canister-analogous" environment, e.g., testing in stainless-steel "mini-canisters" under helium cover gas. Measuring yields under conditions that are very similar to the in-canister environment should help to obtain values close to those that will occur in-canister. In addition, the radiolytic H_2 generation is primarily reported in terms of the total H_2 yield from the sample (generally in µmol) along with specification of experimental conditions including total sample mass and surface area, oxidation mass gain and/or oxide thickness of the sample, and the absorbed radiation dose (in Gy, measured via Fricke dosimetry and adjusted for the aluminum metal). (The mass of water is not reported, because the water in these radiolysis tests generally consists of physisorbed layers that cannot be readily quantified.) Providing these separate pieces of data decouples the reported yields from a specific G-value definition, while providing the data required to calculate a G-value if desired. Where possible, direct comparisons are drawn between similar samples (e.g., nominally identical coupons corroded under the same conditions) to assess the impact of different experimental conditions, in order to minimize confounding variables such as different metal-to-oxide ratios.

5.0 Conclusions

G-values, i.e., the amount of a species produced or consumed by radiolysis normalized by the amount of absorbed radiation energy, are a common way to report radiolysis yields. Despite the seemingly straightforward definition, calculating G-values for a system with more than one material requires a decision of what absorbed energy to use in the calculation, particularly for samples including materials that do not undergo radiolysis but may transfer a portion of their absorbed energy to another material and alter its radiolysis behavior. Differences in G-value definition can complicate direct comparisons between the results of different studies.

Various studies in the literature have investigated the radiolytic breakdown of water or organic compounds in contact with oxide powders, often measuring the radiolytic yield of H_2. Although the oxides do not contain hydrogen themselves, they can increase or decrease the radiolytic H_2 of the overall system. Commonly used approaches for these systems are 1) defining the G-value based on energy deposition in the entire sample and 2) defining the G-value based only on energy deposited directly in the species undergoing radiolysis, e.g., water. The former approach yields relatively low G-values because some of the energy deposited in the oxide remains in the oxide without contributing to radiolysis, while the latter yields relatively high G-values because it does not include the "extra" energy transferred from the oxide. G-values based on only a portion of the sample are also sensitive to the quantification of the different components; for adsorbed species in particular, it can be challenging to accurately quantify the small mass of adsorbed species. This usually involves heating of the samples to high temperature to desorb anything already on the surface of the oxide followed by a controlled exposure to the absorbate of interest. However, not all materials can be heated to high temperature without significantly altering the sample, and the conditions required to fully remove adsorbates vary.

Materials such as (oxy)hydroxides and hydrates add an additional complication since they can undergo radiolysis and generate H_2 themselves as well as host adsorbed water. In addition, they may dehydrate at high temperatures, limiting the options for eliminating or measuring the adsorbed water without altering the material.

Some mixed-material systems such as oxides with water or organic compounds or aluminum coupons with adherent (oxy)hydroxides have shown non-linear yield vs. dose curves, indicating their G-values are not constant. This further complicates the G-value definition, since the G-value obtained will depend on whether it is calculated from the cumulative yield and dose since the start of the experiment (corresponding to an average yield vs. dose slope) or based on the local generation rate (corresponding to the local slope of the yield vs. dose curve), and also limits the G-value's usefulness for models/predictions, since a given amount of dose absorbed to the system cannot be assumed to always produce the same radiolytic yield. Accurately modeling a variable G-value would require characterization of its value over different conditions and likely identification of physical mechanisms underlying the changing yield behavior.

The G-value representation therefore appears to have the most value for application to single components with linear yield vs. dose curves. Unfortunately, there is not a straightforward replacement metric for systems with non-linear yield curves and mixed-material systems. Effectively capturing and predicting their yield behavior will require more detailed consideration of interactions between materials (e.g., energy transfer, relative masses/geometry of the different materials, etc.), potential sources of the radiolysis product (e.g., water vapor, physisorbed water, AlOOH, $Al(OH)_3$), and physical mechanisms that could drive the changes in generation rate/G-values (e.g., potential depletion of certain materials due to radiolytic breakdown) rather than applying a simple normalization by dose. Due to this complexity, it is helpful for radiolysis studies to report their data in a way that allows future readers to analyze the data in different ways beyond the form (e.g., G-values or yields per sample mass) chosen by the authors. For example, reporting unnormalized radiolytic yields along with details of the sample composition/preparation such as

sample mass and corrosion mass gain allows for conversion of the data to yields or G-values normalized by either sample mass or oxide mass.

G-values measured for surrogate coupons resembling the cladding of aluminum-clad spent nuclear fuel (ASNF), i.e., aluminum metal with adherent (oxy)hydroxide films, were compared to selected data from previous literature for mixtures of Al_2O_3 powder with water and for aluminum (oxy)hydroxides in powder form. G-values for Al_2O_3 powder and water were converted from a water basis ($G(H_2)_{H2O}$) to a total sample basis (oxide plus water, $G(H_2)_{mix}$) to enable the comparison. For ASNF surrogate coupons with bayerite ($Al(OH)_3$), the $G(H_2)_{oxide}$ values based on energy deposition in the bayerite film were larger than $G(H_2)_{mix}$ based on an Al_2O_3 powder and adsorbed water mixed sample by up to ~21x but smaller than $G(H_2)_{H2O}$ based on just the adsorbed water in the same Al_2O_3-water mix. $G(H_2)_{oxide}$ for the aluminum coupons with bayerite was larger than $G(H_2)_{oxide}$ for boehmite powders irradiated under argon by up to 35x. Given the differences in the oxide materials (Al_2O_3 vs. AlOOH vs. $Al(OH)_3$) and sample morphology (powder vs. adherent film on metal) and that the $Al(OH)_3$ can also contribute to the radiolytic H_2 yield, the magnitudes of these G-values appear reasonably consistent.

6.0 References

[1] M. M. Riegel, T. T. Truong, 2022, "Technology Maturation Roadmaps for Electrolytic Dissolution of Non-Aluminum Spent Nuclear Fuel (NASNF) at the Savannah River Site," SRNL-L3100-2022-00042.

[2] E. Eidelpes, J. Jarrell, R. Sindelar, 2021, "Technical Basis for Extended Dry Storage of Aluminum-Clad Spent Nuclear Fuel," Idaho National Laboratory, INL/EXT-21-65214.

[3] K. Wefers, C. Misra, 1987, "Oxides and hydroxides of aluminum," Alcoa Technical Paper #19, Alcoa Laboratories Pittsburgh, PA.

[4] A. L. d'Entremont, R. L. Sindelar, 2023, "Review and Summary of Oxide Thickness Data for Aluminum-Clad Spent Nuclear Fuel," Savannah River National Laboratory, SRNL-STI-2023-00038.

[5] A. d'Entremont, R. Smith, C. Rirschl, K. Waldrop, D. Dunn, R. Einzinger, R. Sindelar, 2023, "Drying of Spent Nuclear Fuel: Considerations and Examples," Nuclear Technology, https://doi.org/10.1080/00295450.2023.2226519.

[6] A. L. d'Entremont, R. Smith, "ASNF Drying Recipe – Review of Data," Savannah River National Laboratory, SRNL-L3110-2022-00006.

[7] R. J. Demuth, A. L. D'Entremont, R. Smith, R. L. Sindelar, T. W. Knight, 2024, "Drying and Analysis of Aluminum (Oxy)hydroxide Films for Dry Storage of Aluminum-Clad Spent Nuclear Fuels," *Nuclear Technology*, DOI: 10.1080/00295450.2024.2312019.

[8] J. W. T. Spinks, R. J. Woods, 1990, *An Introduction to Radiation Chemistry*, 3rd ed., John Wiley & Sons, Inc.

[9] N. G. Petrik, A. B. Alexandrov, A. I. Vall, 2001, "Interfacial Energy Transfer during Gamma Radiolysis of Water on the Surface of ZrO_2 and Some Other Oxides," *J. Phys. Chem. B* 105, pp. 5935-5944.

[10] J. M. Caffrey, Jr, A. O. Allen, 1958, "Radiolysis of Pentane Adsorbed on Mineral Solids," *The Journal of Physical Chemistry* 62, pp. 33-37.

[11] J. W. Sutherland, A. O. Allen, 1960, "Radiolysis of Pentane in the Adsorbed State," *Journal of the American Chemical Society* 83, pp. 1040-1047.

[12] J. G. Rabe, B. Rabe, A. O. Allen, 1966, "Radiolysis and Energy Transfer in the Adsorbed State" *The Journal of Physical Chemistry* 70, pp. 1098-1107.

[13] R. R. Hentz, 1964, "Radiation-Induced Reactions of Isopropylbenzene on Silica-Alumina," *The Journal of Physical Chemistry* 68(10), pp. 2889-2894.

[14] J. A. LaVerne, L. Tandon, 2003, "H_2 Production in the Radiolysis of Water on UO_2 and Other Oxides," *J. Phys. Chem. B* 107, pp. 13623-13628.

[15] J. A. LaVerne, L. Tandon, 2002, "H_2 Production in the Radiolysis of Water on CeO_2 and ZrO_2," *J. Phys. Chem. B* 106, pp. 380-386.

[16] J. A. LaVerne, 2005, "H_2 Formation from the Radiolysis of Liquid Water with Zirconia," *J. Phys. Chem. B* 109, pp. 5395-5397.

[17] S. C. Reiff, J. A. LaVerne, 2015, "Gamma and He Ion Radiolysis of Copper Oxides," *J. Phys. Chem. C* 119, pp. 8821−8828.

[18] S. C. Reiff, J. A. LaVerne, 2017, "Radiolysis of water with aluminum oxide surfaces," *Radiation Physics and Chemistry* 131, pp. 46-50.

[19] J. A. LaVerne, L. Tandon, 2005, "H_2 and Cl_2 Production in the Radiolysis of Calcium and Magnesium Chlorides and Hydroxides," *J. Phys. Chem. A* 109, pp. 2861-2865.

[20] M. L. Westbrook, R. L Sindelar, D. L. Fisher, 2015, "Radiolytic hydrogen generation from aluminum oxyhydroxide solids: theory and experiment," *J. Radioanal. Nucl. Chem.* 303, pp. 81–86.

[21] T. A. Yamamoto, S. Seino, M. Katsura, K. Okitsu, R. Oshima, Y. Nagata, 1999, "Hydrogen Gas Evolution from Alumina Nanoparticles Dispersed in Water Irradiated with γ-Ray," *NanoStructured Materials* 12, pp. 1045-1048.

[22] S. Seino, T.A. Yamamoto, R. Fujimoto, K. Hashimoto, M. Katsura, S. Okuda, K. Okitsu, R. Oshima, 2001, "Hydrogen Evolution from Water Dispersing Nanoparticles Irradiated with Gamma-Ray/Size Effect and Dose Rate Effect," *Scripta Mater*. 44, pp. 1709–1712.

[23] E. H. Parker-Quaife, G. P. Horne, C. R. Heathman, C. Verst, P. R. Zalupski, 2019, "Radiation-Induced Molecular Hydrogen Gas Generation by Pre-Corroded Aluminum Alloy 1100," INL/EXT-19-55202, Rev. 1.

[24] G. P. Horne, J. K. Conrad, T. M. Copeland-Johnson, A. Khanolkar, C. D. Pilgrim, J. R. Wilbanks, C. Rae, E. H. Parker-Quaife, 2021, "Milestone 1.2.9: Radiolytic Gas Generation Measurements from Helium-Backfilled Samples of AA1100 and AA6061 Coupons," Idaho National Laboratory, INL/EXT-21-65356.

[25] G. P. Horne, J. K. Conrad, T. M. Copeland-Johnson, X. Pu, A. Khanolkar, J. R. Wilbanks, C. D. Pilgrim, 2022, "Milestone 1.2.10: Steady-state H_2 'roll over' point data for aluminum alloys 1100 and 6061," Idaho National Laboratory, INL/RPT-22-68379.

[26] C. Verst, 2024, "Final Mini-Canister Results Summary," Savannah River National Laboratory, SRNL-L3110-2024-00004.

[27] A. L. d'Entremont, C. G. Verst, 2024, "'Mini-Canister' Radiolysis Testing of ASNF Materials and Surrogates," Savannah River National Laboratory, SRNL-STI-2024-00359.

[28] R. L. Kesterson, R. L. Sindelar, C. G. Verst, G. P. Horne, E. H. Parker-Quaife, 2020, "Evaluation of Radiolysis Data for Hydrogen Gas Generation During Gamma Irradiation of Pre-Corroded and Pristine Aluminum Samples – An Aluminum SNF Dry Storage Study Interim Report," Savannah River National Laboratory, SRNL-STI-2020-00147.